ACS APPLIED MATERIALS & INTERFACES

www.acsami.org

Research Article

All-Nanofiber Network Structure for Ultrasensitive Piezoresistive Pressure Sensors

Yue Zhou, Liupeng Zhao, Wei Tao, Tianshuang Wang, Peng Sun,* Fangmeng Liu, Xu Yan, and Geyu Lu*

Cite This: https://doi.org/10.1021/acsami.1c24257

Read Online

ACCESS | Metrics & More | Article Recommendations | Supporting Information

ABSTRACT: Sensing materials with fiber structures are excellent candidates for the fabrication of flexible pressure sensors due to their large specific surface area and abundant contact points. Here, an ultrathin, flexible piezoresistive pressure sensor that consists of a multilayer nanofiber network structure prepared via a simple electrospinning technique is reported. The ultrathin sensitive layer is composite nanofiber films composed of poly (3,4-ethylenedioxythiophene):poly (styrenesulfonate) and polyamide 6 (PEDOT:PSS/PA6) prepared by simultaneous electrospinning. PEDOT:PSS conductive fibers and PA6 elastic fibers are interwoven to form a multilayer network structure that can achieve ultrahigh sensitivity by forming a wealth of contact points during loading. In particular, gold-deposited PA6 fibers as upper and lower flexible electrodes can effectively increase the initial resistance. Due to this special fiber electrode structure, the sensor is able to generate a large electrical signal variability when subjected to a weak external force. The devices with different sensing properties can be obtained by controlling the electrospinning time. The sensor based on the PEDOT:PSS/PA6 nanofiber network has high sensitivity (6554.6 kPa^{-1} at 0−1.4 kPa), fast response time (53 ms), and wide detection range (0−60 kPa). Significantly, the device maintains ultrahigh sensitivity when cyclically loaded over 10,000 cycles at 5 kPa, which makes it have great prospects for applications in human health monitoring and motion monitoring.

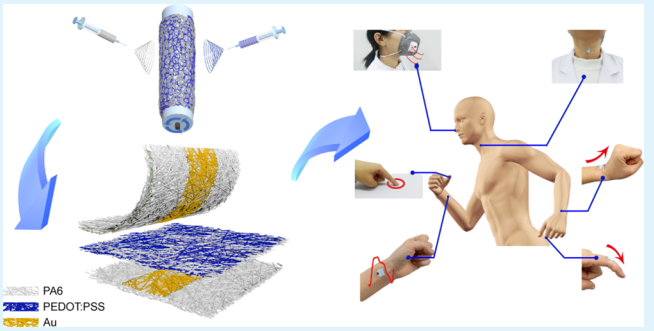

KEYWORDS: *all-nanofiber network, conductive polymers, electrospinning, flexible devices, piezoresistive pressure sensors, health monitoring*

INTRODUCTION

In recent years, flexible wearable technologies have been developed for healthcare, prosthetics, robotics, artificial intelligence, and other fields.[1] In particular, flexible pressure sensors have been widely researched for their promising applications in E-skin,[2] human−computer interactions,[3] health monitoring, and medical diagnosis due to their softness, thinness, and compatibility.[1] Pressure sensors can directly transform the external stimuli into electrical signals for output, which can be divided into four types, including piezoresistive,[4−13] piezocapacitive,[14−17] piezoelectric, and frictional−electric.[18] Among them, the widely investigated piezoresistive devices have the advantages of simple structure[6,13] (mainly composed of flexible electrodes and elastic conductive materials), good performance (e.g., high sensitivity and wide detection range) and easy signal acquisition. Common elastic substrates with low modulus of elasticity (e.g., polyurethane (PU),[19] polyamide 6 (PA6),[20] polyvinyl alcohol (PVA),[21] polyacrylonitrile (PAN),[9] etc.) are soft and easily deformed. The conductive filler with excellent electrical conductivity is assembled with an elastic substrate to form elastic conductive materials. Typical conductive fillers include carbon-based fillers (e.g., carbon black (CB), carbon nanotubes,[10,22,23] graphene),[24,25] metal nanowires (AgNWs),[20] conductive polymers (e.g., polypyrrole (PPy),[26] polyaniline (PANI),[27] and poly(3,4-ethylenedioxythiophene):poly(styrenesulfonate) (PEDOT:PSS)).[28] Poly(3,4-ethylenedioxythiophene) (PEDOT) is a p-type conductive polymer that can achieve high conductivity particle suspensions in water by doping with polystyrene sulfonate (PSS). PEDOT:PSS has promising film formation capabilities, high conductivity, environmental stability, and tunable conductivity and is commonly used to fabricate sensor electrodes and strain sensors[19] by spin-coating or dip-coating. Due to the integrity and limited mechanical flexibility of PEDOT:PSS films ($\varepsilon_{max} \approx 4\%$),[28] there are few studies on pressure sensors based on it, and more other structures of PEDOT:PSS deserve to be explored.

Received: December 15, 2021
Accepted: April 11, 2022

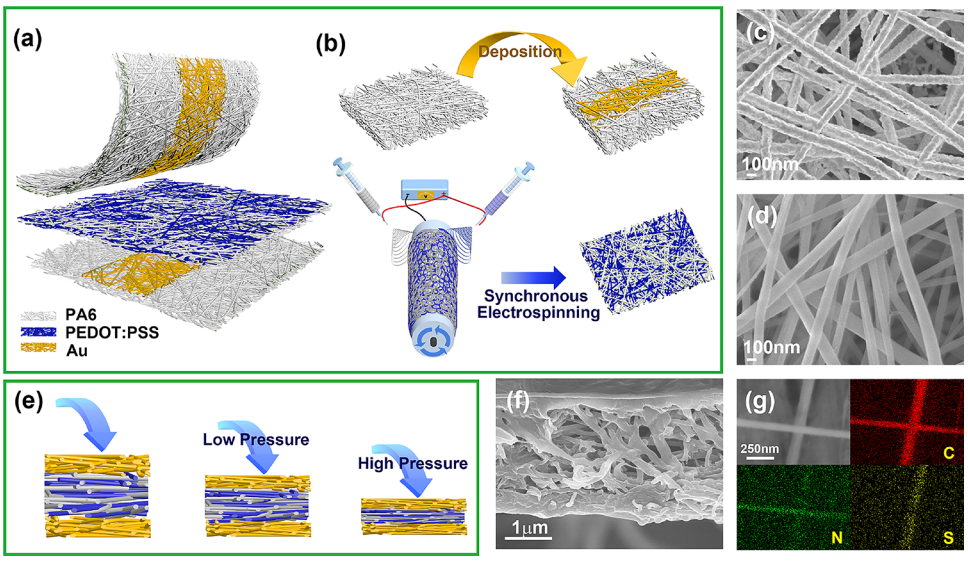

Figure 1. Morphological structure and sensing mechanism of the piezoresistive pressure sensor based on PEDOT:PSS/PA6 fibers. (a) Sandwich structure schematic of the piezoresistive pressure sensor based on PEDOT:PSS/PA6 fiber with gold electrodes. (b) Schematic diagram of the process of preparing patterned gold electrodes and simultaneous electrospinning process for the preparation of PEDOT:PSS/PA6 fibers. (c) SEM image of PA6 fiber after Au deposition. (d) Surface SEM image of PEDOT:PSS/PA6 fibers. (e) Sensing mechanism of the piezoresistive pressure sensor based on PEDOT:PSS/PA6 fibers. (f) Cross-sectional SEM image of PEDOT:PSS/PA6 fibers. (g) EDS elemental mapping images of PEDOT:PSS/PA6 fibers.

To improve the performance of piezoresistive pressure sensors, in addition to the selection of suitable elastic substrates and conductive fillers, various microstructures or nanoscale geometries have been constructed, for example, microstructures (e.g., micropyramid arrays,[6] microcolumn arrays,[7] and micro-hemisphere arrays),[8] porous structures (e.g., sponge-like structures),[29] and nanonetwork structures (e.g., nanofibers,[30] fabrics,[10] etc.). The nanofiber structure with high flexibility and thinness as well as abundant contact points is well suited for the fabrication of high sensitivity and rapid response flexible wearable pressure sensors.[31]

In this work, we report an ultrasensitive and ultrathin flexible pressure sensor consisting of a multilayer nanofiber network prepared via a facile electrospinning technique. The pressure sensor consists of gold-deposited PA6 nanofiber networks as upper and lower flexible electrodes as well as a sensing layer composed of a PEDOT:PSS/PA6 composite nanofiber network. The PEDOT:PSS fibers as a conductive filler with PA6 fibers interwoven in the composite nanofiber network to form a conductive pathway. The sensor displays a large variation in electrical signal when subjected to a weak external force, thus showing an ultrahigh sensitivity (6554.6 kPa^{-1} at 0−1.4 kPa) and fast response (53 ms). Due to the high mechanical strength and good toughness, the as-prepared PA6 fibers result in better flexibility and durability of the sensor. Moreover, as a skeleton, it protects the internal conductive pathway and electrodes, ensuring that the sensor can vary linearly with the pressure in a wide range (0−60 kPa). Importantly, the flexible pressure sensor composed of all-fiber is more comfortable to fit than other structures and can be easily connected to various parts of the body for real-time monitoring of physiological and motion signals, showing great potential for future medical diagnostics.

RESULTS AND DISCUSSION

Figure 1a shows a simple structural schematic of the sensor. It is a typical sandwich structure with three layers of nanofiber network films all prepared by electrospinning. The upper and lower electrodes are nanofiber electrodes obtained by depositing gold on PA6 films, and the sensing layer is a composite nanofiber of PEDOT:PSS and PA6 prepared by simultaneous electrospinning. The experimental procedure is schematically shown below (Figure 1b), where on both sides of the cylindrical collection device are the precursors of PEDOT:PSS and PA6, respectively, both of which are spun simultaneously at the same voltage. Due to the poor viscosity of the conductive polymer PEDOT:PSS, we prepared the obtained PEDOT:PSS fibers with the help of the organic polymer polyethylene oxide (PEO).[32] The formulation of the PA6 fibers is the same as the substrate used for the preparation of the electrodes, which enables to obtain soft and wear-resistant homogeneous fibers very easily. PEDOT:PSS and PA6 fibers are randomly distributed on a high-speed rotating collection device interwoven to form an intermediate layer with both certain electrical conductivity and elasticity, which can be bent and twisted at will and restore the original appearance (Figure S1). The surface and cross-sectional scanning electron micrographs (Figure 1d,f) were examined to observe the morphology and distribution of the fibers, and both fibers were observed to form uniform bead-free fibers with similar diameters of about 100 nm. The structure allows each fiber to be uniformly stressed when subjected to external forces. The thickness and initial resistance of the films in the composite nanofiber network can be controlled by adjusting the electrospinning time. We performed electrospinning for 2, 4, and 6 h to obtain PEDOT:PSS/PA6 films with thicknesses of 1.5, 4, and 7 μm, respectively (Figure S2). Since both fibers are morphologically similar, to further observe the two fibers, we have plotted the distribution of the C, N, and S elements in the fibers by EDS diagram as follows (Figure 1g), in which the origin of the N element is from PA6 and the origin of the S element is from PEDOT:PSS. The results show that the C element is uniformly distributed in each fiber, while the N and the S elements are distributed in different fibers. This indicates

https://doi.org/10.1021/acsami.1c24257
ACS Appl. Mater. Interfaces XXXX, XXX, XXX−XXX

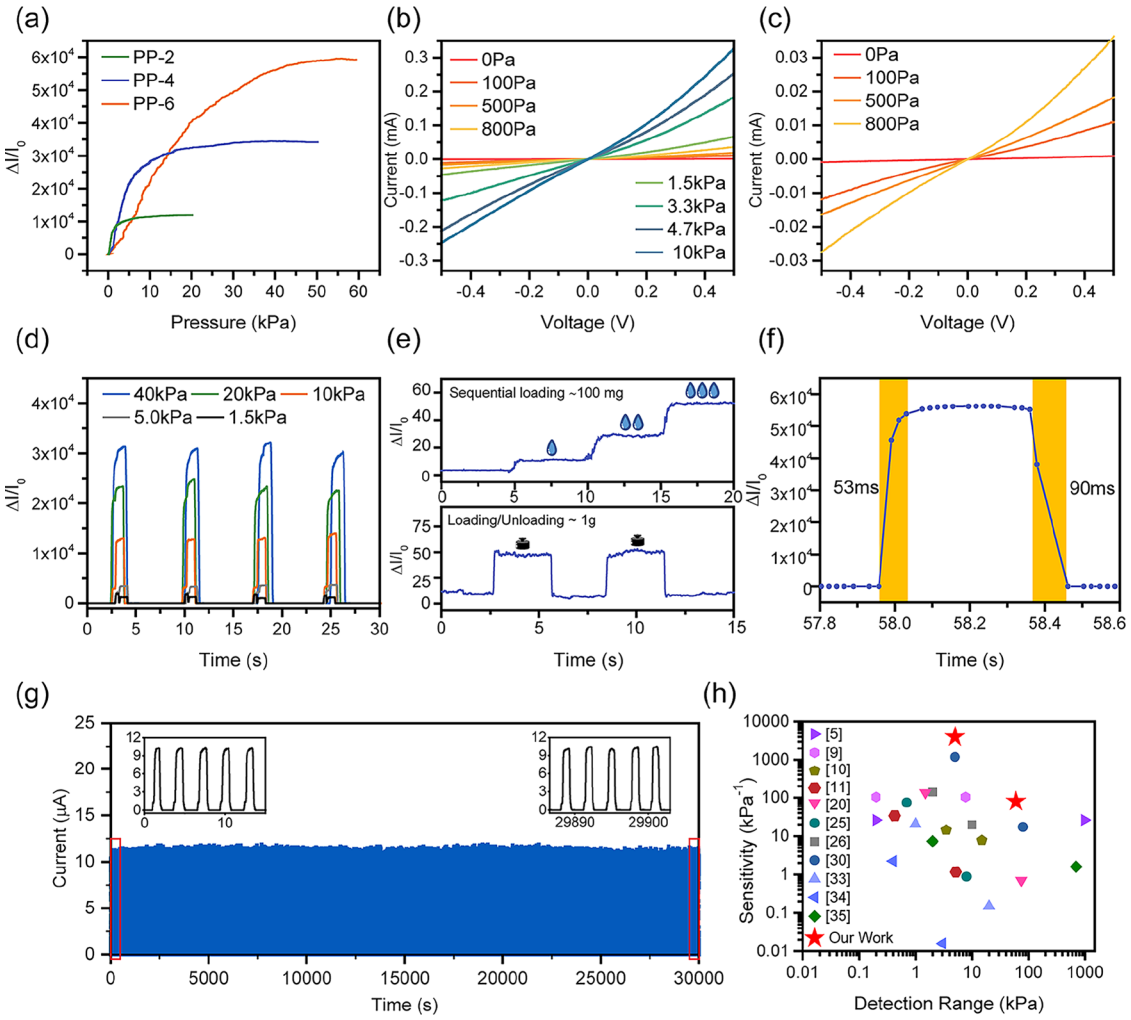

Figure 2. Sensing performance of piezoresistive pressure sensors based on PEDOT:PSS/PA6 fibers. (a) Relative variation curves of current with pressure of electrospinning devices (PP-2, PP-4, and PP-6) for the 2, 4 and 6 h of dynamic loading with different pressures. (b, c) Current−voltage curves of PP-4 devices measured at various pressures from 0 to 10 kPa. (d) Relative change curve of current of the PP-4 device when loading/unloading pressure from 1.5 to 40 kPa in sequence. (e) Top: Relative change curve of current of successive drops of water (about 100 mg) on the PP-4 device. Bottom: Relative change curve of current of loading and unloading a 1 g weight on the PP-4 device. (f) Transient response indication response (53 ms) and recovery (90 ms) times for loading/unloading pressure of the PP-4 device. (g) Variation of the current of the PP-4 device at a pressure of 5 kPa for 10,000 repeated loading cycles. Inset: Current variation during initial and termination phases. (h) Performance comparison between our work and the reported piezoresistive pressure sensors with a fiber network structure.

that our two fibers are not fused with each other but are randomly interwoven together in separate presence. In addition to the design of the sensitive layer structure, the design of the electrodes of flexible fiber structure further enhances the sensitivity of our device. The electrodes with flexibility were obtained by depositing about 100 nm thick gold on the prepared fibers of PA6 (Figure 1b). The scanning electron micrographs of the electrodes (Figure 1c and Figure S4) show that after depositing gold on PA6 nanofibers, the pore structure of the fiber network can be retained intact, the fiber diameter becomes slightly larger, and the surface roughness increases. More details of the experiments will be described in the Experimental Section. In conclusion, we have successfully fabricated a flexible pressure sensor consisting of a multilayer fiber network structure.

The all-fiber-based pressure sensor has a large specific surface area for each layer and an abundance of contact points to have an excellent performance of ultrahigh sensitivity and fast response. Figure 1e shows the sensing mechanism of the pressure sensor based on PEDOT:PSS/PA6 fibers at different stages after being subjected to pressure. The sensing mechanism can be briefly described as follows: In the case of unloading, due to the uneven fiber structure of the electrode and intermediate layer surfaces, there are few conductive paths between the electrode and the intermediate layer without close-fitting. Also, the PEDOT:PSS fibers of the middle layer are interspersed with PA6 fibers at this time, and there are a lot of gaps in the multilayer network structure, resulting in fewer contact points between the conductive fibers (PEDOT:PSS); thus, we can obtain a large initial resistance. As the load increases, the upper and lower electrodes can have contact with the middle layer with a slight external force leading to a rapid decrease in resistance. By further increasing the pressure, the middle layer starts to be compressed and the voids in the nanofiber network gradually become less. Meanwhile, the contact points between the PEDOT:PSS fibers increase, the structural components become tighter, and more conductive pathways are formed. Under high pressure, when all the voids

https://doi.org/10.1021/acsami.1c24257
ACS Appl. Mater. Interfaces XXXX, XXX, XXX−XXX

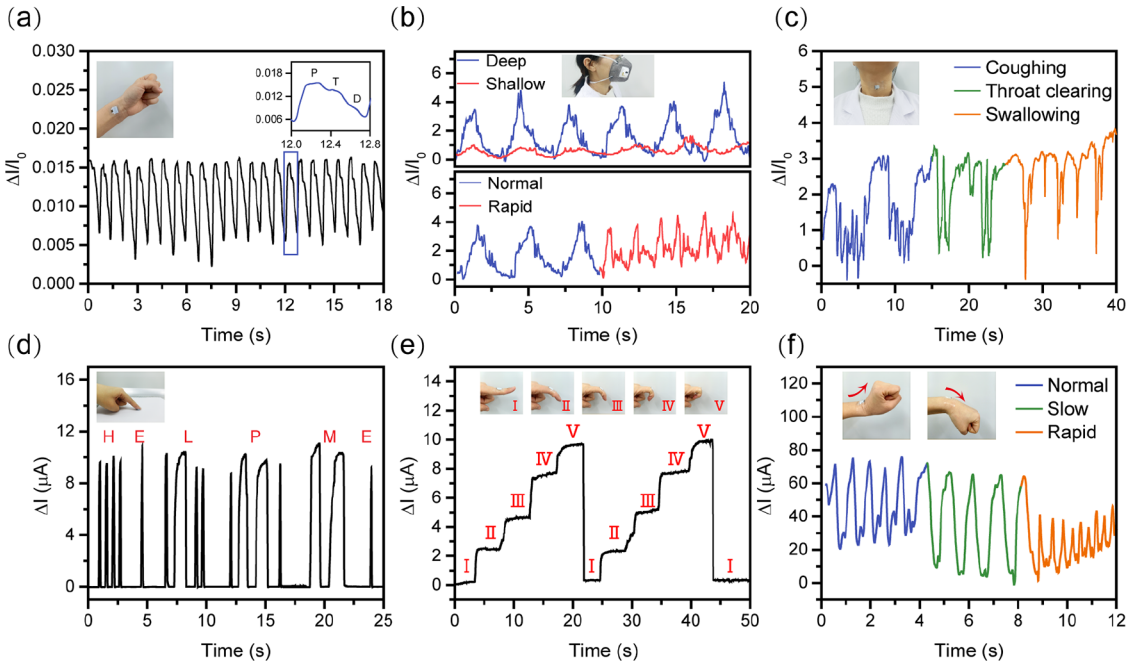

Figure 3. Practical application of piezoresistive pressure sensors based on PEDOT:PSS/PA6 fibers in health monitoring. (a) Monitoring of radial artery pulse waveform in volunteers at rest. Inset, left: photograph of the sensor attached at the wrist; right: magnified view of the pulse waveform showing its characteristic peaks (main, anterior, and posterior micropeaks). (b) Top: Monitoring the relative change curves of sensor current signal in deep breathing and shallow breathing modes in volunteers. Bottom: relative change curves of sensor current signal in normal breathing and fast breathing modes of the monitoring volunteers. Inset: photograph of the volunteer wearing a 3M mask with a sensor at the air valve. (c) Monitoring the relative change curve of the sensor current signal when the volunteer coughs, clears his throat, and swallows. Inset, photograph of the sensor attached to the throat of the volunteer's neck. (d) Sending international Morse code (HELP ME) by taps and long presses on the desktop. Inset: photograph of a sensor attached to the fingertip tapping on the desktop. (e) Monitoring of knuckle flexion movements from 0−120°. Inset: photographs of the sensor attached to the volunteer's index finger joint at different angles. (f) Monitoring of different frequencies of wrist joint oscillation. Inset: photographs of the sensor attached to the wrist joint motion of the volunteer.

between the fibers disappear, the current change also tends to saturate.

We have tested the pressure sensing performance of the pressure sensors fabricated from the PEDOT:PSS/PA6 composite fiber network obtained at different electrospinning times. The current value output with external force was obtained by providing the device with a very low DC voltage (0.1 V) during the test. Figure 2a illustrates the relative variation curves of current values of devices made with electrospun 2, 4, and 6 h intermediate layers (defined as PP-2, PP-4, and PP-6, respectively) when loaded with different pressures. The sensitivity is defined as $S = \frac{(I - I_0)/I_0}{P}$, where $(I - I_0)$ is the amount of current change, I_0 is the current value when no load is applied, I is the current value when subjected to a certain pressure, and P is the pressure applied. We calculated the sensitivity of PP-2, PP-4, and PP-6 devices according to the definition of sensitivity. Table S1 displays the sensitivity and fitted curve parameters of each device in different linear sensing ranges. It can be observed that the sensitivity of PP-2 is high in the low-pressure range (0−1.4 kPa) at about 6554 kPa^{-1}, yet the saturation is easily reached. In contrast, the sensitivity of PP-6 is relatively low, yet it can detect in the wide range of 0−60 kPa. The result is due to the fact that when the interlayer is thin, it is easily compressed by external forces making the PEDOT:PSS fibers contact each other to saturate with a small force. As the thickness of the interlayer increases, the force required for compression increases, but the sensitivity decreases. Five samples of each thickness of the device were taken for testing to ensure reproducibility. The electrical response curves of the fifteen samples with pressure are shown in Figure S5. The sensing performance is generally consistent except for minor deviations introduced by hand. We can choose the appropriate sensitivity and test range for different tests according to the actual application. After that, we have chosen PP-4 for further pressure sensing tests. In order to verify the contribution of the fiber-structured flexible electrodes design to the sensitivity, we replaced the fiber-structured electrodes with flat electrodes in the same sensitivity test. Figure S6 shows the sensitivity curves of PP-4 at the two structured electrodes. As can be easily seen, the electrode structure increases the sensitivity by a factor of 100 (detailed reference at Table S2). Figure 2b,c shows the current−voltage curves of PP-4 under different loads. The increasing slope of the curve with increasing load indicates the formation of good Ohmic contact between the electrodes and the sensitive layer. Moreover, the resistance decreases with increasing pressure, which is the same mechanism as the one we have discussed. We have also performed repeated loading tests under different pressures. Figure 2d shows the current change values under pressures from 1.5 to 40 kPa, which indicates that the sensors can exhibit stable signal output and repeatability. The above test shows that the sensor can maintain a stable current output under both dynamic loading and static loading. One of the distinctive features of the nanofiber structure is the abundance of contact points, which are capable of producing deformation when subjected to very weak pressure. In order to test the sensing characteristics of the sensor for slight pressure, we placed a small weight (1 g) on

https://doi.org/10.1021/acsami.1c24257
ACS Appl. Mater. Interfaces XXXX, XXX, XXX−XXX

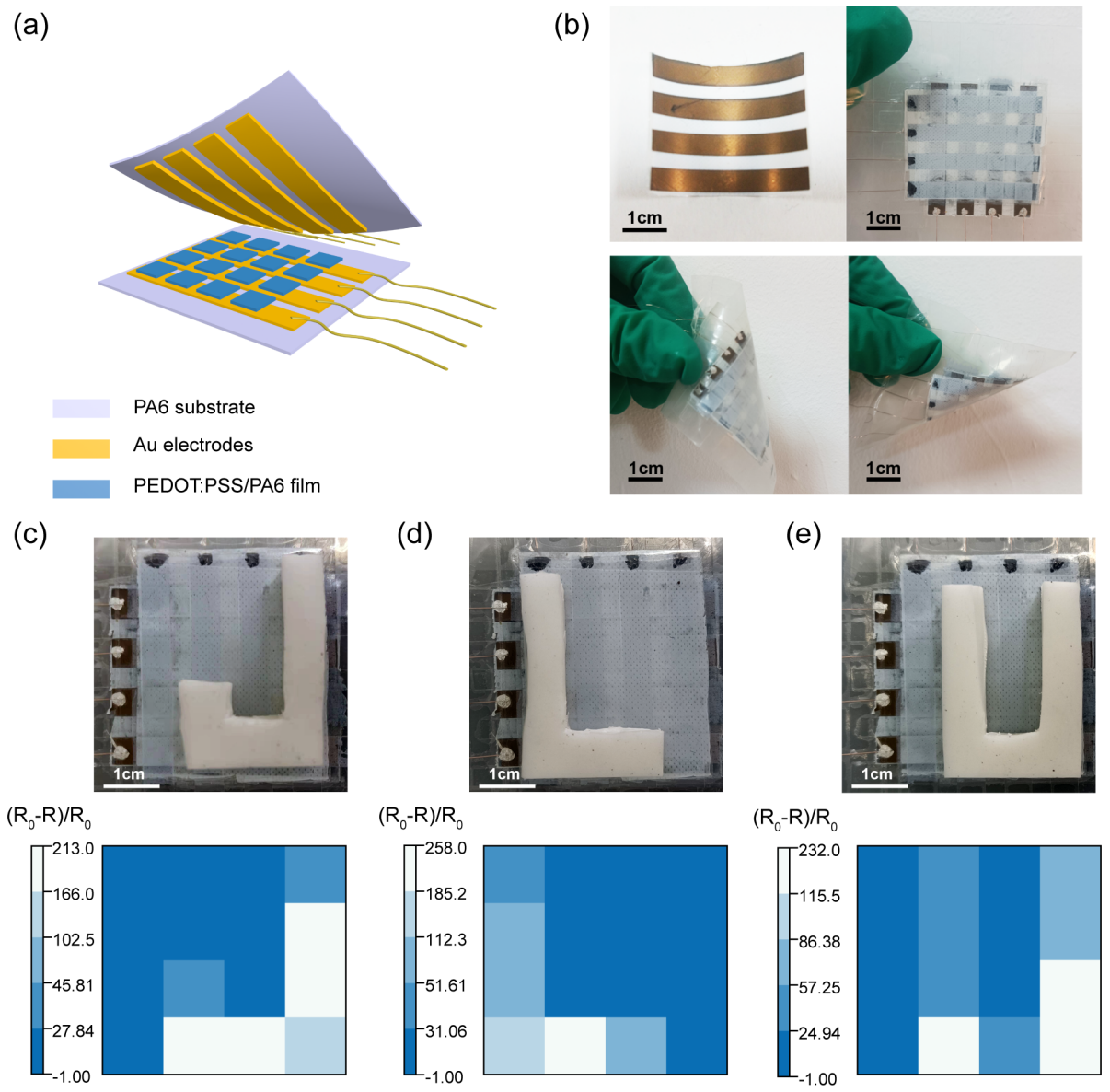

Figure 4. (a) Schematic diagram of the structure of the 4 × 4 flexible sensor array. (b) Photographs of gold electrodes with patterns and 4 × 4 flexible sensor array. (c–e) Photographs of the rubber letters placed on the 4 × 4 flexible sensor array and the corresponding resistance change diagram.

the sensor, and the current value showed a steady change (Figure 2e). When we loaded a drop of water (about 100 mg) in turn, corresponding to a pressure of 20 Pa, the current value increased continuously and steadily with the increase of the drop of water (Figure 2e). We preloaded a slide on the sensor during the test, and the slide served two purposes: completing the contact between the electrodes and the sensitive layer and keeping the sensor uniformly stressed. The experimental results indicate that the sensor is able to detect the small force well. With a pressure sensor consisting of only three layers of nanofibers, it can respond quickly during loading and unloading pressure as shown in Figure 2f. It has a response time of 53 ms and a recovery time of 90 ms to enable real-time pressure measurement. Figure 2g shows the change of the current for a cyclic loading of more than 10,000 cycles at a pressure of 5 kPa. The magnified graphs of the beginning and end show no drift in the current values. Figure S7 shows the change of current when we cyclically loaded 25 kPa for 3000 cycles. Compared with the initial time, there is a slight increase of current after 3000 cycles, which may be due to the fatigue of the fiber structure. However, the sensor still maintains a high sensitivity, indicating that the sensor has great durability and repeatability with a long working life. Such excellent performance is mainly due to the fact that both the electrodes and the sensing layer of the sensor contain PA6 fibers with good mechanical properties. Figure S8 shows the stress–strain curves of the electrodes and the sensing layer. The SEM images of the electrodes and sensing layer after stretching and compressing are shown in Figure S9. There is essentially no change in morphology after stretching and compression. Therefore, the sensor maintains its original mechanical strength even after repeated loading. The all-fiber-based pressure sensor has achieved an ultrahigh sensitivity of 6554 kPa^{-1} and is able to be tested in the range of 0–60 kPa. Our work is also outstanding compared to the reported piezoresistive pressure sensors with fiber network structure as

https://doi.org/10.1021/acsami.1c24257
ACS Appl. Mater. Interfaces XXXX, XXX, XXX–XXX

shown in Figure 2h.[5,9−11,20,25,26,30,33−35] The materials and sensing performance of the recently reported piezoresistive pressure sensors based on the fiber network structure is listed in Table S3.

Moreover, we have placed the sensors under relative humidities (RH) of 56, 77, and 99% and tested the sensing performance of the sensors under a complex high humidity environment. Figures S10 and S11 show that the sensitivity of the sensor does not change with increasing humidity. This is due to the encapsulation of the device with a waterproof polyurethane (PU) film, which effectively insulates water molecules from the environment. As a result of this packaging, the PEDOT:PSS is not affected by the environmental humidity, thus ensuring high sensing performance of the sensor in high humidity environments. The electrical properties of the elastic conductive composites could sometimes be dependent on the AC frequency.[36] To characterize the electrical properties of PEDOT:PSS/PA6-based fiber films at AC frequency, we measured the impedance spectrum of the sensor from 10 to 10^6 Hz. The curves of AC conductivity and phase angle with frequency are shown in Figure S12. It demonstrates that the AC conductivity is almost independent of frequency in the low-frequency range. The phase angle is also close to $\theta \approx 0°$, exhibiting resistive characteristics.

The results of the above pressure sensing tests have shown that the PEDOT:PSS/PA6 pressure sensor has excellent sensing performance and great potential for the health monitoring of weak physiological signals and the sports of body joints. We fixed the sensor to the wrist with 3M medical tape to record the real-time human pulse signal (Figure 3a). Due to the fast response and recovery time, it is possible to obtain the detailed structure of the pulse waveform. Three different peaks are exhibited in a pulse waveform, including the percussion (P), tidal (T), and diastolic (D) peaks.[37] Based on the waveforms useful information about the blood vessels can be provided. For example, the radial enhancement index (AI = T/P) can be easily derived from the P and T waves in normal conditions (Figure 3a, inset; female AI = 0.816; normal range for adult females is 81.1 ± 16.1%), which can show arterial stiffness conditions. It is a preliminary assessment for the current state of suboptimal health in young people and the prevention of diseases such as atherosclerosis. The sensor was fixed at the outlet valve of the KN95 mask to monitor breathing through the nose (Figure 3b). We tested the different states of normal breathing, high-frequency breathing, deep breathing, and shallow breathing. The respiratory intensity is too high in patients with metabolic acidosis caused by uremia, diabetes, etc. and too low in patients who are dying. The normal breathing rate of adults is 16−20 times per minute. In medicine when the breathing rate is abnormal, there may be fever, anemia, hypoxia or poisoning, intracranial diseases,[38] etc. The sensor can perform respiratory monitoring in real time according to the current response changes to achieve timely detection of related diseases. The weak vibrations in the throat can also be detected using the as-fabricated sensors. When we performed the actions of coughing, swallowing, and throat clearing separately, different shapes of signal output can be observed (Figure 3c). Therefore, it can be applied to medical diagnosis by transmitting the signal of the patient's eating and drinking behaviors in real-time to assist doctors in assessing the oropharyngeal function of patients with swallowing disorders.[39] In addition to the physiological microsignal, the sensor can quickly generate a corresponding signal when tapped on the table by fixing it at the finger. We have sent the Morse code "HELP ME" using taps and long presses (Figure 3d). The results indicated that we can achieve the use of the finger to send Morse code to help Parkinson's patients who have difficulty moving other parts of their body to communicate simply. As the sensor has a wide detection range, it can also detect the sports of joints, such as finger joints, wrist joints, etc. We fixed the sensor at the finger joints (Figure 3e). When we bent the finger 0, 30, 60, 90, and 120 degrees, the current value gradually increased, and when the finger returned to 0 degrees, the current signal can also be quickly recovered and has good repeatability. When the sensor was fixed at the wrist joint (Figure 3f) and oscillated at different frequencies, the current response changed accordingly. Based on these tests, we can assist in the examination of joint recovery therapy for patients with movement disorders by tracking human joint movements in real time as well as initially detect joint development in infants and children.[40]

The PEDOT:PSS/PA6 composite fiber films can be easily cut to various sizes to make large-area sensor arrays for pressure spatial sensing. We cut the film to a size of 5 mm × 5 mm and sandwiched them between vertically placed electrodes to make a 4 × 4 sensor array with an area of 4 mm × 4 mm per pixel as shown in Figure 4a and Figure S13. Figure 4b shows photographs of the gold electrodes with patterns and the 4 × 4 flexible sensor array, which can be visualized as we random bend. When we placed the rubber-made capital letters "J," "L," and "U" (JI LIN UNIVERSITY) on the sensor array (Figure 4c−e), the corresponding pixel point will exhibit a change in current value. Such large-area pressure sensor arrays are expected to be used in the future for applications such as human−computer interactions.

CONCLUSIONS

In conclusion, we have designed a ultrathin, flexible piezoresistive pressure sensor with ultrahigh sensitivity based on the all-fiber network structure by electrospinning technology. In our work, the special sensitive layer consists of two different fibers (conductive fibers: PEDOT:PSS; elastic fibers: PA6) with a large specific surface area, which provides abundant contact sites. Simultaneously, a fiber network electrode is designed to further increase the initial resistance and thus improve the sensitivity. Furthermore, we could fabricate different sensitivity and detection ranges of the sensors by adjusting the electrospinning time. The experimental results indicate that we have obtained sensors with ultrahigh sensitivity (6554 kPa^{-1}) and wide detection range (0−60 kPa). Interestingly, the pressure sensor based on the PEDOT:PSS/PA6 composite fiber network structure has important applications in health monitoring (e.g., human physiological signals and operational joint signals, etc.) and spatial pressure identification on the basis of their excellent performance. The results of our work will be of great value for flexible wearable devices in medical diagnosis, human−computer interactions, etc.

EXPERIMENTAL SECTION

Materials. Poly(3,4-ethylenedioxythiophene):poly(styrenesulfonate) (PEDOT: PSS) (Clevios PH1000) was purchased from Heraeus Precious. Polyamide 6 (PA6), polyethylene oxide (PEO) (M_w = 900, 000), and N, N-dimethylformamide (DMF) were

https://doi.org/10.1021/acsami.1c24257
ACS Appl. Mater. Interfaces XXXX, XXX, XXX−XXX

purchased from Sigma-Aldrich. Formic acid was purchased from Aladdin. All chemicals were used without further purification.

Fabrication of PEDOT:PSS/PA6 Films and Au/PA6 Electrodes. The precursor of PEDOT:PSS was prepared by dissolving 0.134 g of PEO in 5.12 g of PEDOT:PSS solution and 0.69 g of DMF under stirring at room temperature for 24 h to obtain a uniformly spinnable solution. The precursor of PA6 was prepared by dissolving 3 g of PA6 granules in formic acid under stirring at room temperature for 12 h to obtain a uniformly spinnable solution with a concentration of 15 wt %. The prepared PEDOT:PSS solution and PA6 solution were loaded into medical syringes for electrospinning connected with 21G and 19G metal needles, respectively. The metal needles were fixed at a distance of 13 and 16 cm on both sides of the cylindrical collecting drum. An electrospinning equipment assembled in the laboratory with a voltage of 16 kV was used for the preparation. The flow rates of PEDOT:PSS and PA6 were fixed at 0.1 and 0.05 mL/h, respectively. During the electrospinning process, temperature and humidity are continuously monitored and controlled within the range of 25 ± 2 °C and 40% RH. The PA6 films used as electrode substrates were prepared by electrospinning the same precursor solution at a flow rate of 0.1 mL/h and a voltage of 20 kV for 2 h. Subsequently, 100 nm of gold was deposited on the prepared PA6 film, and gold electrodes with mask patterns were obtained.

Fabrication of the Flexible PEDOT:PSS/PA6 Pressure Sensor and the 4 × 4 Sensing Array. During the single-sensor fabrication, two pieces of PA6/Au films (size: 5 mm × 10 mm) were attached to a waterproof 3M medical dressing as electrode backup. Then, the copper wires were attached to the end of the gold electrodes with silver paste to lead the wires. The PEDOT:PSS/PA6 film with the size of 7 mm × 7 mm was removed from the collector using a PET frame with double-sided tape. The prepared PEDOT:PSS/PA6 film was positioned on top of the electrode, and the other electrode was placed perpendicular to the bottom electrode at the top with the crossed area as the sensing zone. Last, the sandwich structure of the sensor is glued together using 3M medical dressing, and it is well encapsulated to insulate it from the outside environment. The method of preparing the 4 × 4 sensing array is the same as mentioned before: we deposited the electrode pattern designed in advance on top of the PA6 film with the size of 5 cm × 5 cm, drew out the electrodes with copper wire, and places the upper and lower electrodes vertically. The 16 pieces of PEDOT:PSS/PA6 films with the size of 6 mm × 6 mm were sandwiched in the middle, and finally, the whole array was encapsulated with a medical dressing.

Characterization. The morphology and structure of the PEDOT:PSS/PA6 films and Au/PA6 films were observed by a field emission scanning electron microscope (FESEM, JSM-7500F JEOL) attached with an energy-dispersive spectroscope (EDS). The electrodynamic force measurement system built in our laboratory consists of an electrodynamic measuring table (ESM303, Mark10) and a digital force gauge (M5-5, Mark10) to perform pressure sensing tests. The current−voltage curves at different loads were measured by an electrochemical workstation. A DC power supply (DPS-305BM) provided 0.1 V to the sensor, and the values of current versus pressure for different thickness devices were recorded with a DMM-6500 digital multimeter.

■ ASSOCIATED CONTENT

Supporting Information

The Supporting Information is available free of charge at https://pubs.acs.org/doi/10.1021/acsami.1c24257.

(Figures S1 and S2) Details of the PEDOT:PSS/PA6 fiber films; (Figure S3) details of the pressure sensor based on the PEDOT:PSS/PA6 fiber films; (Figure S4) morphology of the Au/PA6 electrodes; (Figure S5) sensitivity testing of different samples of three different thickness devices; (Figure S6) sensitivity testing of the devices with different types of electrodes; (Figure S7) durability testing of the sensors under high pressure; (Figure S8) mechanical properties of the Au/PA6 films and the PEDOT:PSS/PA6 composite films; (Figure S9) morphology of the Au/PA6 films and the PEDOT:PSS/PA6 composite films after stretching and compression; (Figure S10 and Figure S11) sensitivity testing of the sensors in high-humidity environments; (Figure S12) AC frequency testing of the sensors; (Figure S13) details on the structure of the 4 × 4 sensor array based on PEDOT:PSS/PA6 fiber films; (Table S1) sensitivity and linear fitting parameters of the PP-2, PP-4, PP-6 devices in various linear sensing ranges; (Table S2) sensitivity and linear fitting parameters of the PP-4 devices with flat- and fiber-structured electrodes in various linear sensing ranges; (Table S3) materials and sensing performance of recently reported piezoresistive pressure sensors based on fiber network structure (PDF)

■ AUTHOR INFORMATION

Corresponding Authors

Peng Sun − *State Key Laboratory of Integrated Optoelectronics, College of Electronic Science and Engineering and International Center of Future Science, Jilin University, Changchun 130012, China;* orcid.org/0000-0002-9509-9431; Email: pengsun@jlu.edu.cn

Geyu Lu − *State Key Laboratory of Integrated Optoelectronics, College of Electronic Science and Engineering and International Center of Future Science, Jilin University, Changchun 130012, China;* orcid.org/0000-0002-7428-2456; Email: lugy@jlu.edu.cn

Authors

Yue Zhou − *State Key Laboratory of Integrated Optoelectronics, College of Electronic Science and Engineering, Jilin University, Changchun 130012, China;* orcid.org/0000-0001-7735-549X

Liupeng Zhao − *State Key Laboratory of Integrated Optoelectronics, College of Electronic Science and Engineering, Jilin University, Changchun 130012, China*

Wei Tao − *State Key Laboratory of Integrated Optoelectronics, College of Electronic Science and Engineering, Jilin University, Changchun 130012, China*

Tianshuang Wang − *State Key Laboratory of Integrated Optoelectronics, College of Electronic Science and Engineering, Jilin University, Changchun 130012, China;* orcid.org/0000-0003-3196-3005

Fangmeng Liu − *State Key Laboratory of Integrated Optoelectronics, College of Electronic Science and Engineering and International Center of Future Science, Jilin University, Changchun 130012, China;* orcid.org/0000-0002-5555-5543

Xu Yan − *State Key Laboratory of Integrated Optoelectronics, College of Electronic Science and Engineering, Jilin University, Changchun 130012, China;* orcid.org/0000-0003-2152-675X

Complete contact information is available at: https://pubs.acs.org/10.1021/acsami.1c24257

Author Contributions

All authors have approved the final version of the manuscript.

Notes

The authors declare no competing financial interest.

https://doi.org/10.1021/acsami.1c24257
ACS Appl. Mater. Interfaces XXXX, XXX, XXX−XXX

■ ACKNOWLEDGMENTS

This work is supported by the National Nature Science Foundation of China (nos. 61833006 and 61831011), the Jilin Province Science and Technology Development Plan Program (no. 20200301010RQ), the project on Industrial Innovation Capability of Jilin Province (no. 2020C048), and the Fundamental Research Funds for the Central Universities and Graduate Interdisciplinary Research Fund of Jilin University (no. 10183201833).

■ REFERENCES

(1) Niu, Y.; Liu, H.; He, R.; Li, Z.; Ren, H.; Gao, B.; Guo, H.; Genin, G. M.; Xu, F. The New Generation of Soft and Wearable Electronics for Health Monitoring in Varying Environment: From Normal to Extreme Conditions. *Mater. Today* **2020**, *41*, 219−242.

(2) Wang, B.; Facchetti, A. Mechanically Flexible Conductors for Stretchable and Wearable E-Skin and E-Textile Devices. *Adv. Mater.* **2019**, 1901408.

(3) Pyo, S.; Lee, J.; Bae, K.; Sim, S.; Kim, J. Recent Progress in Flexible Tactile Sensors for Human-Interactive Systems : From Sensors to Advanced Applications. *Adv. Mater.* **2021**, 2005902.

(4) Wang, D.; Zhou, X.; Song, R.; Fang, C.; Wang, Z.; Wang, C.; Huang, Y. Freestanding Silver/Polypyrrole Composite Film for Multifunctional Sensor with Biomimetic Micropattern for Physiological Signals Monitoring. *Chem. Eng. J.* **2021**, *404*, No. 126940.

(5) Lee, S.; Reuveny, A.; Reeder, J.; Lee, S.; Jin, H.; Liu, Q.; Yokota, T.; Sekitani, T.; Isoyama, T.; Abe, Y.; Suo, Z.; Someya, T. A Transparent Bending-Insensitive Pressure Sensor. *Nat. Nanotechnol.* **2016**, *11*, 472−478.

(6) Pyo, S.; Lee, J.; Kim, W.; Jo, E.; Kim, J. Multi-Layered, Hierarchical Fabric-Based Tactile Sensors with High Sensitivity and Linearity in Ultrawide Pressure Range. *Adv. Funct. Mater.* **2019**, *29*, 1−9.

(7) Li, W.; Jin, X.; Han, X.; Li, Y.; Wang, W.; Lin, T.; Zhu, Z. Synergy of Porous Structure and Microstructure in Piezoresistive Material for High-Performance and Flexible Pressure Sensors. *ACS Appl. Mater. Interfaces* **2021**, *13*, 19211−19220.

(8) Wang, X.; Tao, L.; Yuan, M.; Wang, Z.; Yu, J.; Xie, D.; Luo, F.; Chen, X.; Wong, C. Sea Urchin-Like Microstructure Pressure Sensors with An Ultra-Broad Range and High Sensitivity. *Nat. Commun.* **2021**, *12*, 1−9.

(9) Huang, Y.; You, X.; Tang, Z.; Tong, K. Y.; Guo, P.; Zhao, N. Interface Engineering of Flexible Piezoresistive Sensors via Near-Field Electrospinning Processed Spacer Layers. *Small Methods* **2021**, *5*, 1−9.

(10) Fu, X.; Wang, L.; Zhao, L.; Yuan, Z.; Zhang, Y.; Wang, D.; Wang, D.; Li, J.; Li, D.; Shulga, V.; Shen, G.; Han, W. Controlled Assembly of MXene Nanosheets As an Electrode and Active Layer for High-Performance Electronic Skin. *Adv. Funct. Mater.* **2021**, 2010533.

(11) Liu, M.; Pu, X.; Jiang, C.; Liu, T.; Huang, X.; Chen, L.; Du, C.; Sun, J.; Hu, W.; Wang, Z. L. Large-Area All-Textile Pressure Sensors for Monitoring Human Motion and Physiological Signals. *Adv. Mater.* **2017**, *29*, 1−9.

(12) Wang, Q.; Jian, M.; Wang, C.; Zhang, Y. Carbonized Silk Nanofiber Membrane for Transparent and Sensitive Electronic Skin. *Adv. Funct. Mater.* **2017**, *27*, 1605657.

(13) Liu, H.; Chen, X.; Zheng, Y.; Zhang, D.; Zhao, Y.; Wang, C.; Pan, C.; Liu, C.; Shen, C. Lightweight, Superelastic, and Hydrophobic Polyimide Nanofiber /MXene Composite Aerogel for Wearable Piezoresistive Sensor and Oil/Water Separation Applications. *Adv. Funct. Mater.* **2021**, 2008006.

(14) Wang, Z.; Si, Y.; Zhao, C.; Yu, D.; Wang, W.; Sun, G. Flexible and Washable Poly(Ionic Liquid) Nanofibrous Membrane with Moisture Proof Pressure Sensing for Real-Life Wearable Electronics. *ACS Appl. Mater. Interfaces* **2019**, *11*, 27200−27209.

(15) Yao, S.; Zhu, Y. Wearable Multifunctional Sensors Using Printed Stretchable Conductors Made of Silver Nanowires. *Nanoscale* **2014**, *6*, 2345−2352.

(16) Lee, S.; Franklin, S.; Hassani, F. A.; Yokota, T.; Nayeem, M. O. G.; Wang, Y.; Leib, R.; Cheng, G.; Franklin, D. W.; Someya, T. Nanomesh Pressure Sensor for Monitoring Finger Manipulation Without Sensory Interference. *Science* **2020**, *370*, 966−970.

(17) You, I.; MacKanic, D. G.; Matsuhisa, N.; Kang, J.; Kwon, J.; Beker, L.; Mun, J.; Suh, W.; Kim, T. Y.; Tok, J. B. H.; Bao, Z.; Jeong, U. Artificial Multimodal Receptors Based on Ion Relaxation Dnamics. *Science* **2020**, *370*, 961−965.

(18) Lee, G.; Son, J. H.; Lee, S.; Kim, S. W.; Kim, D.; Nguyen, N. N.; Lee, S. G.; Cho, K. Fingerpad-Inspired Multimodal Electronic Skin for Material Discrimination and Texture Recognition. *Adv. Sci.* **2021**, 2002606.

(19) Ding, Y.; Xu, W.; Wang, W.; Fong, H.; Zhu, Z. Scalable and Facile Preparation of Highly Stretchable Electrospun PEDOT:PSS@PU Fibrous Nonwovens toward Wearable Conductive Textile Applications. *ACS Appl. Mater. Interfaces* **2017**, *9*, 30014−30023.

(20) Li, X.; Fan, Y. J.; Li, H. Y.; Cao, J. W.; Xiao, Y. C.; Wang, Y.; Liang, F.; Wang, H. L.; Jiang, Y.; Wang, Z. L.; Zhu, G. Ultracomfortable Hierarchical Nanonetwork for Highly Sensitive Pressure Sensor. *ACS Nano* **2020**, *14*, 9605−9612.

(21) Li, X.; Li, X.; Lu, Y.; Shang, C.; Ding, X.; Zhang, J.; Feng, Y.; Xu, F. Wearable, Washable, and Highly Sensitive Piezoresistive Pressure Sensor Based on a 3D Sponge Network for Real-Time Monitoring Human Body Activities. *ACS Appl. Mater. Interfaces* **2021**, *13*, 46848−46857.

(22) Cao, R.; Pu, X.; Du, X.; Yang, W.; Wang, J.; Guo, H.; Zhao, S.; Yuan, Z.; Zhang, C.; Li, C.; Wang, Z. L. Screen-Printed Washable Electronic Textiles As Self-Powered Touch/Gesture Tribo-Sensors for Intelligent Human-Machine Interaction. *ACS Nano* **2018**, *12*, 5190−5196.

(23) Du, D.; Tang, Z.; Ouyang, J. Highly Washable E-Textile Prepared by Ultrasonic Nanosoldering of Carbon Nanotubes onto Polymer Fibers. *J. Mater. Chem. C* **2018**, *6*, 883−889.

(24) Niu, F.; Qin, Z.; Min, L.; Zhao, B.; Lv, Y.; Fang, X.; Pan, K. Ultralight and Hyperelastic Nanofiber-Reinforced MXene−Graphene Aerogel for High-Performance Piezoresistive Sensor. *Adv. Mater. Technol.* **2021**, *2100394*, 1−8.

(25) Ren, H.; Zheng, L.; Wang, G.; Gao, X.; Tan, Z.; Shan, J.; Cui, L.; Li, K.; Jian, M.; Zhu, L.; Zhang, Y.; Peng, H.; Wei, D.; Liu, Z. Transfer-Medium-Free Nanofiber-Reinforced Graphene Film and Applications in Wearable Transparent Pressure Sensors. *ACS Nano* **2019**, *13*, 5541−5548.

(26) Pan, H.; Xie, G.; Pang, W.; Wang, S.; Wang, Y.; Jiang, Z.; Du, X.; Tai, H. Surface Engineering of a 3D Topological Network for Ultrasensitive Piezoresistive Pressure Sensors. *ACS Appl. Mater. Interfaces* **2020**, *12*, 38805−38812.

(27) Chen, W.; Wang, Z.; Li, Q.; Jin, X.; Liu, H.; Zhou, H. Hollow Polyaniline Microsphere Functionalized Paper with Multimodal Sensitivity to Strain, Humidity, and Pressure. *ACS Appl. Electron. Mater.* **2020**, *2*, 247−253.

(28) Wang, Y.; Zhu, C.; Pfattner, R.; Yan, H.; Jin, L.; Chen, S.; Molina-Lopez, F.; Lissel, F.; Liu, J.; Rabiah, N. I.; Chen, Z.; Chung, J. W.; Linder, C.; Toney, M. F.; Murmann, B.; Bao, Z. A Highly Stretchable, Transparent, and Conductive Polymer. *Sci. Adv.* **2017**, *3*, 1−11.

(29) Zhong, W.; Liu, C.; Liu, Q.; Piao, L.; Jiang, H.; Wang, W.; Liu, K.; Li, M.; Sun, G.; Wang, D. Ultrasensitive Wearable Pressure Sensors Assembled by Surface-Patterned Polyolefin Elastomer Nanofiber Membrane Interpenetrated with Silver Nanowires. *ACS Appl. Mater. Interfaces* **2018**, *10*, 42706−42714.

(30) Wang, Z.; Zhang, L.; Liu, J.; Li, C. A Flexible Bimodal Sensor Based on an Electrospun Nanofibrous Structure for Simultaneous Pressure-Temperature Detection. *Nanoscale* **2019**, *11*, 14242−14249.

(31) Ghosh, R.; Pin, K. Y.; Reddy, V. S.; Jayathilaka, W. A. D. M.; Ji, D.; Serrano-García, W.; Bhargava, S. K.; Ramakrishna, S.; Chinnappan, A. Micro/Nanofiber-Based Noninvasive Devices for

https://doi.org/10.1021/acsami.1c24257
ACS Appl. Mater. Interfaces XXXX, XXX, XXX−XXX

Health Monitoring Diagnosis and Rehabilitation. *Appl. Phys. Rev.* **2020**, *7*, 041309.
(32) Bessaire, B.; Mathieu, M.; Salles, V.; Yeghoyan, T.; Celle, C.; Simonato, J. P.; Brioude, A. Synthesis of Continuous Conductive PEDOT: PSS Nanofibers by Electrospinning: A Conformal Coating for Optoelectronics. *ACS Appl. Mater. Interfaces* **2017**, *9*, 950−957.
(33) Qi, K.; He, J.; Wang, H.; Zhou, Y.; You, X.; Nan, N.; Shao, W.; Wang, L.; Ding, B.; Cui, S. A Highly Stretchable Nanofiber-Based Electronic Skin with Pressure-, Strain-, and Flexion-Sensitive Properties for Health and Motion Monitoring. *ACS Appl. Mater. Interfaces* **2017**, *9*, 42951−42960.
(34) Gao, X.; Zhou, F.; Li, M.; Wang, X.; Chen, S.; Yu, J. Flexible Stannum-Doped $SrTiO_3$ Nano fi ber Membranes for Highly Sensitive and Reliable Piezoresistive Pressure Sensors. *ACS Appl. Mater. Interfaces* **2021**, *13*, 52811−52821.
(35) Chen, T.; Zhang, S. H.; Lin, Q. H.; Wang, M. J.; Yang, Z.; Zhang, Y. L.; Wang, F. X.; Sun, L. N. Highly Sensitive and Wide-Detection Range Pressure Sensor Constructed on a Hierarchical-Structured Conductive Fabric As a Human-Machine Interface. *Nanoscale* **2020**, *12*, 21271−21279.
(36) Yan, X.; Bowen, C. R.; Yuan, C.; Hao, Z.; Pan, M. Carbon Fibre Based Flexible Piezoresistive Composites to Empower Inherent Sensing Capabilities for Soft Actuators. *Soft Matter* **2019**, *15*, 8001−8011.
(37) Kohara, K.; Tabara, Y.; Oshiumi, A.; Miyawaki, Y.; Kobayashi, T.; Miki, T. Radial augmentation index: A Useful and Easily Obtainable Parameter for Vascular Aging. *Am. J. Hypertens.* **2005**, *18*, 11−14.
(38) Marik, P. E.; Kaplan, D. Aspiration Pneumonia and Dysphagia in the Elderly. *Chest* **2003**, *124*, 328−336.
(39) Laptook, A. R. Neurologic and Metabolic Issues in Moderately Preterm, Late Preterm, and Early Term Infants. *Clin. Perinatol.* **2013**, *40*, 723−738.
(40) Watanabe, H.; Hamada, Y.; Toshima, T.; Nagasawa, K. Conservative Treatment for Trigger Thumb in Children. *Arch. Orthop., Traum. Surg.* **2001**, *121*, 388−390.

https://doi.org/10.1021/acsami.1c24257
ACS Appl. Mater. Interfaces XXXX, XXX, XXX−XXX